

Ruthenium Complexes with Tetraphenylimidodiphosphinate: Syntheses, Structures, and Applications to Catalytic Organic Oxidation

Wai-Man Cheung, Ho-Yuen Ng, Ian D. Williams, and Wa-Hung Leung*

Department of Chemistry, The Hong Kong University of Science and Technology, Clear Water Bay, Kowloon, Hong Kong, People's Republic of China

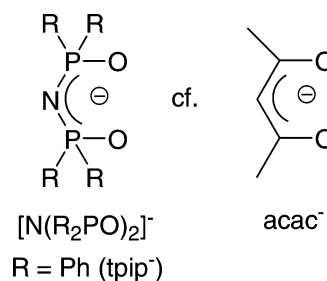
Received January 4, 2008

Treatment of $\text{Ru}(\text{PPh}_3)_3\text{Cl}_2$ with $\text{K}(\text{tpip})$ ($\text{tpip}^- = [\text{N}(\text{Ph}_2\text{PO})_2]^-$) afforded $\text{Ru}(\text{tpip})(\text{PPh}_3)_2\text{Cl}$ (**1**), which reacted with 4-*t*-Bu- $\text{C}_6\text{H}_4\text{CN}$, $\text{SO}_2(\text{g})$, and $\text{NH}_3(\text{g})$ to give $\text{Ru}(\text{tpip})(\text{PPh}_3)_2\text{Cl}(4\text{-}t\text{-BuC}_6\text{H}_4\text{CN})$ (**2**), $\text{Ru}(\text{tpip})(\text{PPh}_3)_2\text{Cl}(\text{SO}_2)$ (**3**), and *fac*- $[\text{Ru}(\text{NH}_3)_3(\text{PPh}_3)_2\text{Cl}][\text{tpip}]$ (**4**), respectively. Reaction of $[\text{Ru}(\text{CO})_2\text{Cl}_2]_x$ with $\text{K}(\text{tpip})$ in refluxing tetrahydrofuran (THF) led to isolation of the K/Ru bimetallic compound $\text{K}_2\text{Ru}_2(\text{tpip})_4(\text{CO})_4\text{Cl}_2$ (**5**). Photolysis of *cis*- $\text{Ru}(\text{tpip})_2(\text{NO})\text{Cl}$ in MeCN and wet CH_2Cl_2 afforded *cis*- $\text{Ru}(\text{tpip})_2(\text{MeCN})\text{Cl}$ (**6**) and *cis*- $\text{Ru}(\text{tpip})_2(\text{H}_2\text{O})\text{Cl}$ (**7**), respectively. Refluxing **6** in neat THF yielded $\text{Ru}(\text{tpip})_2(\text{THF})\text{Cl}$ (**8**). Treatment of $\text{Ru}(\text{CHR})\text{Cl}_2(\text{PCy}_3)_2$ ($\text{Cy} = \text{cyclohexyl}$) with $[\text{Ag}(\text{tpip})_4]$ afforded *cis*- $\text{Ru}(\text{tpip})_2(\text{CHR})(\text{PCy}_3)$ [$\text{R} = \text{Ph}$ (**9**), OEt (**10**)]. Complex **9** is capable of catalyzing oxidation of alcohols and olefins with *N*-methylmorpholine *N*-oxide and iodosylbenzene, respectively. The crystal structures of **2–7** and **9** were determined.

Introduction

Ru complexes in oxygen-rich ligand environments are of interest because they are relevant to the active sites of oxide-based heterogeneous Ru catalysts, which have found applications in organic oxidations.¹ In order to gain insight into the molecular mechanisms of oxide-supported Ru catalysts, we sought to investigate the organometallic chemistry of Ru compounds containing oxygen donor ligands. We were particularly interested in π -donating phosphinate ligands that are compatible with both hard and soft metal centers. Previous studies demonstrated that the facially coordinated tris(phosphinate) ligands $[(\eta^5\text{-C}_5\text{H}_5)\text{Co}\{\text{P}(\text{O})(\text{OR})_2\}_3]^-$ can stabilize low-valence organoruthenium^{2,3} as well as high-valence Ru oxo⁴ and nitrido⁵ complexes. To further explore the organometallic chemistry of chelating phosphinate ligands, we set out to synthesize Ru complexes with bidentate imidodiphosphinate ligands.

Chart 1



Imidodiphosphinates $[\text{N}(\text{R}_2\text{PO})_2]^-$ (Chart 1), such as tetraphenylimidodiphosphinate ($\text{R} = \text{Ph}$) or tpip^- , which are considered to be inorganic analogues of acetylacetonates (acac^-), can form stable complexes with a variety of metals.⁶ Metal- tpip complexes have received much attention recently because of their applications as NMR shift agents,⁷ lumi-

* To whom correspondence should be addressed. E-mail: chleung@ust.hk.

(1) See for example: (a) Yamaguchi, K.; Mori, K.; Mizugaki, T.; Ebitani, K.; Kaneda, K. *J. Am. Chem. Soc.* **2000**, *122*, 7144. (b) Matsushita, T.; Ebitani, K.; Kaneda, K. *Chem. Commun.* **1999**, 265. (c) Yamaguchi, K.; Mizuno, N. *Chem.—Eur. J.* **2003**, *9*, 4353. (d) Wu, D. L.; Wight, A. P.; Davis, M. E. *Chem. Commun.* **2003**, 758. (e) Tada, M.; Coquet, R.; Yoshida, J.; Kinoshita, M.; Iwasawa, Y. *Angew. Chem., Int. Ed.* **2007**, *46*, 7220. (f) Cheung, W.-H.; Yu, W.-Y.; Yip, W.-P.; Zhu, N.-Y.; Che, C.-M. *J. Org. Chem.* **2002**, *67*, 7716.

(2) Kläui, W. *Angew. Chem., Int. Ed. Engl.* **1990**, *29*, 627.

(3) (a) Leung, W.-H.; Chan, E. Y. Y.; Williams, I. D.; Wong, W.-T. *Organometallics* **1997**, *16*, 3234. (b) Leung, W.-H.; Chan, E. Y. Y.; Wong, W.-T. *Organometallics* **1998**, *17*, 1245.

(4) (a) Power, J. M.; Evertz, K.; Henling, L.; Marsh, R.; Schaefer, W. P.; Labinger, J. A.; Bercaw, J. E. *Inorg. Chem.* **1990**, *29*, 5058. (b) Kelson, E. P.; Henling, L. M.; Schaefer, W. P.; Labinger, J. A.; Bercaw, J. E. *Inorg. Chem.* **1993**, *32*, 2863.

(5) Yi, X.-Y.; Lam, T. C. H.; Sau, Y.-K.; Zhang, Q.-F.; Williams, I. D.; Leung, W.-H. *Inorg. Chem.* **2007**, *46*, 7193.

(6) (a) Haiduc, I. In *Comprehensive Coordination Chemistry II*; McCleverty, J. A., Meyer, T. J., Eds.; Elsevier Pergamon: Amsterdam, 2003; Vol. 1, p 323. (b) Ly, T. Q.; Woollins, J. D. *Coord. Chem. Rev.* **1998**, *176*, 451.

nescent materials,⁸ and catalysts for organic oxidations.⁹ While main-group, lanthanide, and early transition-metal complexes with tpip^- have been well documented, relatively few late transition-metal- tpip complexes have been isolated.⁶ To our knowledge, organoruthenium compounds containing tpip^- are unknown to date. This is in sharp contrast to the well-explored $\text{Ru}(\text{acac})_2$ system, whose members exhibit interesting redox¹⁰ and organometallic chemistry¹¹ and can serve as building blocks for coordination polymers.^{10a,12} Vaissermann and co-workers^{9a,b} reported that Ag(I) - and Cu(II) - tpip complexes can catalyze aerobic co-oxidation of hydrocarbons and aldehydes, demonstrating that tpip^- is stable toward oxidants and thus may find applications in organic oxidations. This prompted us to investigate the catalytic activity of $\text{Ru}(\text{tpip})$ complexes in organic oxidations. Herein we describe the synthesis, crystal structures, and electrochemistry of mono- and bis(tpip) complexes of Ru and their applications in catalytic oxidation of alcohols and olefins.

Experimental Section

General Considerations. All manipulations were carried out under nitrogen by standard Schlenk techniques. Solvents were purified, distilled, and degassed prior to use. NMR spectra were recorded using a Bruker ARX 300 or Varian Mercury 300 spectrometer operating at 300, 75.5, 121.5, and 282.5 MHz for ^1H , ^{13}C , ^{31}P , and ^{19}F , respectively. Chemical shifts (δ , ppm) were reported with reference to SiMe_4 (^1H and ^{13}C), H_3PO_4 (^{31}P), and $\text{CF}_3\text{C}_6\text{H}_5$ (^{19}F). Infrared spectra were recorded using a PerkinElmer 16 PC FT-IR spectrophotometer and mass spectra using a Finnigan TSQ 7000 spectrometer. Cyclic voltammetry was performed using a Princeton Applied Research (PAR) model 273A potentiostat. The working and reference electrodes were glassy carbon and Ag/

AgNO_3 (0.1 M in MeCN), respectively. Potentials were reported with reference to the ferrocenium/ferrocene ($\text{Cp}_2\text{Fe}^{+/0}$) couple. Elemental analyses were performed by Medac Ltd. (Surrey, U.K.).

$\text{K}(\text{tpip})$,¹³ $[\text{Ag}(\text{tpip})]_4$,^{9a} $\text{Ru}(\text{PPh}_3)_3\text{Cl}_2$,¹⁴ $[\text{Ru}(\text{CO})_2\text{Cl}_2]_x$,¹⁵ $\text{cis-Ru}(\text{tpip})_2(\text{NO})\text{Cl}$,¹⁶ and $\text{Ru}(\text{CHR})(\text{PCy}_3)_2\text{Cl}_2$ (Cy = cyclohexyl, R = Ph, OEt)¹⁷ were prepared according to literature methods. Other reagents were purchased from commercial sources and used as received.

Preparation of $\text{Ru}(\text{tpip})(\text{PPh}_3)_2\text{Cl}$ (1). A suspension of $\text{Ru}(\text{PPh}_3)_3\text{Cl}_2$ (96 mg, 0.10 mmol) and 1 equiv of $\text{K}(\text{tpip})$ (46 mg, 0.10 mmol) in THF (10 mL) was heated at reflux for 3 h. The solvent was pumped off, and the residue was washed with Et_2O . Recrystallization from $\text{CH}_2\text{Cl}_2/\text{hexane}$ afforded dark-brown crystals. Yield: 91 mg, 85%. ^1H NMR (CDCl_3): δ 6.82–7.48 (m, 40H). $^{31}\text{P}\{^1\text{H}\}$ NMR (CDCl_3): δ 28.35 (s, tpip), 64.73 (s, PPh_3). Anal. Calcd for $\text{C}_{60}\text{H}_{50}\text{ClINO}_2\text{P}_4\text{Ru}\cdot\text{H}_2\text{O}$: C, 65.8; H, 4.8; N, 1.3. Found: C, 65.9; H, 4.6; N, 1.2.

Preparation of $\text{Ru}(\text{tpip})(\text{PPh}_3)_2(4\text{-}t\text{-Bu-C}_6\text{H}_4\text{CN})\text{Cl}$ (2). To a solution of **1** (40 mg, 0.037 mmol) in CH_2Cl_2 was added 1 drop of 4-*tert*-butylbenzonitrile. The pale-brown solution turned yellow immediately. The solvent was pumped off, and the residue was washed with hexane. Recrystallization from $\text{CH}_2\text{Cl}_2/\text{hexane}$ afforded yellowish-orange crystals. Yield: 30 mg, 65%. ^1H NMR (CDCl_3): δ 1.28 (s, 9H, *t*-Bu), 6.37 (d, J = 8.4 Hz, H_m of 4-*t*-Bu- $\text{C}_6\text{H}_4\text{CN}$), 7.08–8.23 (m, 52H). $^{31}\text{P}\{^1\text{H}\}$ NMR (CDCl_3): δ 23.97 (d, J = 3.3 Hz, tpip^-), 51.18 (d, J = 3.3 Hz, PPh_3). IR (KBr) ν_{CN} (cm^{-1}): 2227. Anal. Calcd for $\text{C}_{71}\text{H}_{63}\text{ClINO}_2\text{P}_4\text{Ru}$: C, 69.0; H, 5.1; N, 2.3. Found: C, 69.0; H, 5.3; N, 2.1.

Preparation of $\text{Ru}(\text{tpip})(\text{PPh}_3)_2(\text{SO}_2)\text{Cl}$ (3). $\text{SO}_2(\text{g})$ was bubbled through a solution of **1** (40 mg, 0.037 mmol) in CH_2Cl_2 (20 mL) for 15 s, during which the solution color changed from pale-brown to orange. The solvent was pumped off, and the residue was washed with hexane. Recrystallization from $\text{CH}_2\text{Cl}_2/\text{hexane}$ afforded orange crystals. Yield: 36 mg, 85%. ^1H NMR (CDCl_3): δ 6.80–7.85 (m, 50H). $^{31}\text{P}\{^1\text{H}\}$ NMR (CDCl_3): δ 27.46 (s, tpip), 32.36 (s, PPh_3). IR (KBr) ν_{SO} (cm^{-1}): 1247. Anal. Calcd for $\text{C}_{60}\text{H}_{50}\text{ClINO}_4\text{P}_4\text{RuS}$: C, 63.1; H, 4.4; N, 1.2. Found: C, 63.0; H, 4.4; N, 1.2.

Preparation of $\text{fac-}[\text{Ru}(\text{NH}_3)_3(\text{PPh}_3)_2\text{Cl}][\text{tpip}]$ (4). $\text{NH}_3(\text{g})$ was bubbled through a solution of **1** (40 mg, 0.037 mmol) in CH_2Cl_2 (20 mL) for 30 s, during which the color of the solution changed from pale-brown to yellowish-green. The solvent was pumped off, and the residue was washed with hexane. Recrystallization from $\text{CH}_2\text{Cl}_2/\text{hexane}$ afforded yellowish-green crystals. Yield: 31 mg, 73%. ^1H NMR (CDCl_3): δ 1.65 (br s, 3H, NH_3), 2.25 (br s, 3H, NH_3), 3.01 (br s, 3H, NH_3), 7.09–7.71 (m, 50H). $^{31}\text{P}\{^1\text{H}\}$ NMR (CDCl_3): δ 11.00 (s, tpip), 50.69 (s, PPh_3). Anal. Calcd for $\text{C}_{60}\text{H}_{59}\text{ClN}_4\text{O}_2\text{P}_4\text{Ru}$: C, 63.9; H, 5.3; N, 5.0. Found: C, 63.4; H, 5.3; N, 5.0.

Preparation of $\text{K}_2\text{Ru}_2(\text{tpip})_4(\text{CO})_4\text{Cl}_2$ (5). A suspension of $[\text{Ru}(\text{CO})_2\text{Cl}_2]_x$ (23 mg, 0.10 mmol) and 2 equiv of $\text{K}(\text{tpip})$ (91 mg, 0.20 mmol) in THF (10 mL) was heated at reflux for 3 h. The solvent was pumped off, and the residue was extracted with Et_2O . Recrystallization from $\text{CH}_2\text{Cl}_2/\text{Et}_2\text{O}/\text{hexane}$ afforded yellow crystals. Yield: 67 mg, 63%. ^1H NMR (CDCl_3): δ 6.74–7.99 (m, 40H). $^{31}\text{P}\{^1\text{H}\}$ NMR (CDCl_3): δ 13.95 (s), 22.03 (s), 30.52 (d, J = 3.6 Hz), 33.58 (d, J = 3.6 Hz). IR (KBr) ν_{CO} (cm^{-1}): 1974, 2051. Anal.

- (7) Barkaoui, L.; Charrouf, M.; Rager, M. N.; Denise, B.; Platzer, N.; Rüdler, R. *Bull. Soc. Chim. Fr.* **1997**, 134, 167.
- (8) (a) Magennis, S. W.; Parsons, S.; Pikramenou, Z. *Chem.—Eur. J.* **2002**, 24, 5761. (b) Magennis, S. W.; Parsons, S.; Corval, A.; Woollins, J. D.; Pikramenou, Z. *Chem. Commun.* **1999**, 61. (c) Bassett, A. P.; Van Deun, R.; Nockemann, P.; Glover, P. B.; Kariuki, B. M.; Van Hecke, K.; Van Meervelt, L.; Pikramenou, Z. *Inorg. Chem.* **2005**, 44, 6140. (d) Glover, P. B.; Bassett, A. P.; Nockemann, P.; Kariuki, B. M.; Van Deun, R.; Pikramenou, Z. *Chem.—Eur. J.* **2007**, 13, 6308.
- (9) (a) Rudler, H.; Denise, B.; Gregorio, J. R.; Vaissermann, J. *Chem. Commun.* **1997**, 2299. (b) Rudler, H.; Denise, B. *J. Mol. Catal. A* **2000**, 154, 277. (c) Yi, X.-Y.; Ng, G. K. Y.; Williams, I. D.; Leung, W.-H. *Inorg. Chim. Acta* **2006**, 359, 3581.
- (10) (a) Hasegawa, T.; Lau, T. C.; Taube, H.; Schaefer, W. P. *Inorg. Chem.* **1991**, 30, 2921. (b) Oomura, K.-i.; Ooyama, D.; Satoh, Y.; Nagao, N.; Nagao, H.; Howell, F. S.; Mukaida, M. *Inorg. Chim. Acta* **1998**, 269, 342. (c) Baird, I. R.; Cameron, B. R.; Skerlj, R. T. *Inorg. Chim. Acta* **2003**, 353, 107. (d) Baird, I. R.; Rettig, S. J.; James, B. R.; Skov, K. A. *Can. J. Chem.* **1999**, 77, 1821. (e) Majumdar, P.; Falvello, L. R.; Tomás, M.; Goswami, S. *Chem.—Eur. J.* **2001**, 7, 5222. (f) Ghumaan, S.; Sarkar, B.; Patra, S.; van Slageren, J.; Fiedler, J.; Kaim, W.; Lahiri, G. K. *Inorg. Chem.* **2005**, 44, 3210. (g) Wu, A.; Masland, J.; Swartz, R. D.; Kaminsky, W.; Mayer, J. M. *Inorg. Chem.* **2007**, 46, 11190. (h) Maji, S.; Sarkar, B.; Mobin, S. M.; Fiedler, J.; Kaim, W.; Lahiri, G. K. *Dalton Trans.* **2007**, 2411.
- (11) (a) Bennett, M. A.; Byrnes, M. J.; Kováčik, I. *J. Organomet. Chem.* **2004**, 689, 4463. (b) Bennett, M. A.; Byrnes, M. J.; Willis, A. C. *Organometallics* **2003**, 22, 1018. (c) Bennett, M. A.; Heath, G. A.; Hockless, D. C. R.; Kovacic, I.; Willis, A. C. *J. Am. Chem. Soc.* **1998**, 120, 932.
- (12) (a) Toma, L. M.; Toma, L. D.; Delgado, F. S.; Ruiz-Pérez, C.; Sletten, J.; Cano, J.; Clemente-Juan, J. M.; Lloret, F.; Julve, M. *Coord. Chem. Rev.* **2006**, 250, 2176. (b) Yeung, W.-F.; Lau, P.-H.; Lau, T.-C.; Wei, H.-Y.; Sun, H.-L.; Gao, S.; Chen, Z.-D.; Wong, W.-T. *Inorg. Chem.* **2005**, 44, 6579.

- (13) Wang, F. T.; Najdzionek, J.; Leneker, K. L.; Wasserman, H.; Braitsch, D. M. *Synth. React. Inorg. Met. Org. Chem.* **1978**, 8, 119.
- (14) Stephenson, T. A.; Wilkinson, G. *Inorg. Nucl. Chem.* **1966**, 28, 945.
- (15) Colton, R.; Farthing, R. H. *Aust. J. Chem.* **1971**, 24, 903.
- (16) Cheung, W.-M.; Zhang, Q.-F.; Lai, C.-Y.; Williams, I. D.; Leung, W.-H. *Polyhedron* **2007**, 26, 4631.
- (17) Schwab, P.; Grubbs, R. H.; Ziller, J. W. *J. Am. Chem. Soc.* **1996**, 118, 100.

Calcd for $C_{100}H_{80}Cl_2K_2N_4O_{12}P_8Ru_2$: C, 56.4; H, 3.8; N, 2.6. Found: C, 56.9; H, 4.0; N, 2.7.

Preparation of *cis*-Ru(tpip)₂(MeCN)Cl (6). A solution of *cis*-Ru(tpip)₂(NO)Cl (30 mg, 0.030 mmol) in CH_2Cl_2 /MeCN (100 mL, 9:1 v/v) was irradiated with UV light (9 W, Hg lamp) for 1 h, during which the pale-purple solution turned yellow. The solvent was removed, and the residue was extracted with CH_2Cl_2 . Recrystallization from CH_2Cl_2 /Et₂O/hexane afforded yellow crystals. Yield: 26 mg, 85%. μ_{eff} ($CDCl_3$, Evans method¹⁸) = 1.7 μ_B . Anal. Calcd for $C_{50}H_{43}ClN_3O_4P_4Ru \cdot CH_2Cl_2$: C, 55.9; H, 4.1; N, 3.8. Found: C, 55.9; H, 4.0; N, 3.8.

Preparation of *cis*-Ru(tpip)₂(H₂O)Cl (7). A solution of *cis*-Ru(tpip)₂(NO)Cl (30 mg, 0.030 mmol) in wet CH_2Cl_2 (100 mL) was irradiated with UV light (9 W, Hg lamp) for 1 h, during which the pale-purple solution turned dark-orange. The solvent was removed, and the residue was extracted with CH_2Cl_2 . Recrystallization from CH_2Cl_2 /Et₂O/hexane in air afforded pale-brown crystals. Yield: 14 mg, 48%. Anal. Calcd for $C_{48}H_{42}ClN_3O_5P_4Ru \cdot \frac{1}{2}H_2O$: C, 57.9; H, 4.4; N, 2.8. Found: C, 57.7; H, 4.2; N, 2.7.

Preparation of *cis*-Ru(tpip)₂(THF)Cl (8). A solution of **6** (30 mg, 0.030 mmol) in THF (10 mL) was heated at reflux overnight, during which the yellow solution turned pale-orange. The solvent was pumped off, and the residue was extracted with Et₂O. Addition of excess hexane afforded an orange solid. Yield: 24 mg, 76%. Anal. Calcd for $C_{52}H_{48}ClN_2O_5P_4Ru$: C, 60.0; H, 4.7; N, 2.7. Found: C, 59.6; H, 4.8; N, 2.4.

Preparation of *cis*-Ru(tpip)₂(CHPh)(PCy₃) (9). To a solution of Ru(=CHPh)(PCy₃)₂Cl₂ (41 mg, 0.050 mmol) in CH_2Cl_2 (10 mL) was added 0.5 equiv of [Ag(tpip)]₄ (52 mg, 0.025 mmol), and the reaction mixture was stirred at room temperature (RT) for 2 h. The solvent was pumped off, and the residue was extracted with CH_2Cl_2 /Et₂O (1:1 v/v). Addition of hexane and concentration to 2 mL afforded green crystals. Yield: 39 mg, 60%. ¹H NMR ($CDCl_3$): δ 1.12–2.36 (m, 33H, Cy), 6.94–7.23 (m, 12H, Ph), 7.29 (t, *J* = 7.7 Hz, 2H, H_m of CHPh), 7.31–7.51 (m, 12H, Ph), 7.70 (t, *J* = 7.7 Hz, 1H, H_p), 8.28–8.83 (m, 16H, Ph), 8.94 (d, *J* = 7.7 Hz, 2H, H_o of CHPh), 22.46 (d, *J* = 7.5 Hz, 1H, CHPh). ³¹P{¹H} NMR ($CDCl_3$): δ 21.84 (m), 26.75 (m), 27.17 (m), 28.06 (s), 34.85 (m). ¹³C{¹H} NMR ($CDCl_3$): δ 295.07 (s, Ru=C). Anal. Calcd for $C_{73}H_{79}N_2O_4P_5Ru$: C, 67.2; H, 6.1; N, 2.2. Found: C, 66.8; H, 6.3; N, 2.2.

Preparation of *cis*-Ru(tpip)₂(CHOEt)(PCy₃) (10). This compound was prepared similarly to **9**, using Ru(=CHOEt)(PCy₃)₂Cl₂ (40 mg, 0.050 mmol) in place of Ru(=CHPh)(PCy₃)₂Cl₂. Yield: 43 mg, 67%. ¹H NMR ($CDCl_3$): δ 0.89 (m, 3H, CH₂CH₃), 1.13–2.56 (m, 33H, Cy), 3.88–1.86 (m, 2H, CH₂CH₃), 6.90–8.43 (m, 40H, Ph), 16.62 (s, 1H, CHPh). ³¹P{¹H} NMR ($CDCl_3$): δ 22.83 (m), 23.12 (m), 27.14 (m), 33.05 (m), 44.62 (s). ¹³C{¹H} NMR ($CDCl_3$): δ 290.60 (d, *J* = 18 Hz, Ru=C). Anal. Calcd for $C_{69}H_{79}N_2O_5P_5Ru \cdot \frac{1}{2}Et_2O$: C, 65.1; H, 6.7; N, 2.1. Found: C, 65.4; H, 6.3; N, 1.8.

Ru-Catalyzed Ring-Closing Metathesis of Diethyl Diallylmalonate. This reaction was carried out according to a literature procedure.¹⁹ To a solution of **9** (4 mg, 0.003 mmol) in $CDCl_3$ (0.5 mL) in a NMR tube was added a 20-fold excess of diethyl diallylmalonate (15 μ L, 0.061 mmol) at room temperature. The progress of the reaction was monitored by ¹H NMR spectroscopy. The percent ring closure was calculated on the basis of the ratio of the amounts of the four β hydrogens in the product (H_p) and starting material (H_s), i.e., % ring closure = H_p/(H_p + H_s).¹⁹

General Procedure for Ru-Catalyzed Oxidation of Alcohols.

The oxidant (0.2 mmol) was added to a solution of Ru catalyst (0.002 mmol) and alcohol (0.08 mmol) in CH_2Cl_2 (2 mL), and the reaction mixture was stirred at room temperature. The organic products were analyzed by GLC using bromobenzene as the internal standard.

General Procedure for Ru-Catalyzed Oxidation of Olefins.

Iodosylbenzene (0.2 mmol) was added to a solution of Ru catalyst (0.002 mmol) and olefin (0.08 mmol) in CH_2Cl_2 (2 mL), and the reaction mixture was stirred at room temperature under nitrogen. The organic products were analyzed by GLC using bromobenzene as the internal standard.

X-ray Crystallography. Details concerning the crystallographic data for complexes **2–7** and **9** are summarized in Table 1. Preliminary examinations and intensity data collection were performed on a Bruker SMART-APEX 1000 area-detector diffractometer using graphite-monochromatized Mo K α radiation (λ = 0.70173 Å). The collected frames were processed using the software SAINT.²⁰ The data were corrected for absorption using the program SADABS. Structures were solved by direct methods and refined by full-matrix least-squares on *F*² using the SHELXTL software package.²¹ Unless stated otherwise, non-hydrogen atoms were refined with anisotropic displacement parameters. Selected bond lengths and angles for complexes **2–7** and **9** are listed in Tables 2–6.

Results and Discussion

Syntheses. A. Ru(II) Complexes. The syntheses of Ru(tpip) complexes are summarized in Scheme 1. Treatment of Ru(PPh₃)₃Cl₂ with K(tpip) in refluxing THF led to isolation of brown crystals analyzed as the mono(tpip) complex Ru(tpip)(PPh₃)₂Cl (**1**). Ru(II)–bis(tpip) complexes could not be isolated even when excess K(tpip) was used, indicating the reluctance of Ru(II) to bind to two hard bis(phosphinate) ligands. It may be noted that similar reactions with analogous chalcogen ligands K[N(R₂PQ)₂] (R = Ph, i-Pr; Q = S, Se) led to formation of the five-coordinate bis(chelate) complexes Ru[N(R₂PQ)₂]₂(PPh₃).²² The ³¹P{¹H} NMR spectrum of **1** displayed two singlets at δ 28.35 and 64.73, which were assigned to the tpip[–] and PPh₃ ligands, respectively. The ³¹P resonance for the tpip[–] ligand was shifted downfield relative to that for K(tpip) (δ 14.2 in $CDCl_3$). A preliminary X-ray diffraction study revealed that **1** is monomeric and has a pseudo-trigonal-bipyramidal structure, with the two PPh₃ ligands and one P=O group in the equatorial plane. Unfortunately, the structure could not be refined satisfactorily because of poor crystal quality.

Compound **1** is stable in the solid state but air-sensitive in solutions. It readily reacts with Lewis bases to give octahedral adducts. For example, treatment of **1** with 4-*tert*-butylbenzonitrile led to isolation of Ru(tpip)(PPh₃)₂Cl(4-*t*-Bu-C₆H₄CN) (**2**). While reaction of **1** with SO₂(g) afforded the sulfur dioxide adduct Ru(tpip)(PPh₃)₂Cl(SO₂) (**3**), reaction with NH₃(g) led to dissociation of the tpip[–] ligand and

(18) Schubert, E. M. *J. Chem. Educ.* **1992**, 69, 62.

(19) Sanford, M. S.; Henling, L. M.; Grubbs, R. H. *Organometallics* **1998**, 17, 5384.

(20) Sheldrick, G. M. *SADABS*; University of Göttingen: Göttingen, Germany, 1997.

(21) Sheldrick, G. M. *SHELXTL-Plus V5.1 Software Reference Manual*; Bruker AXS Inc.: Madison, WI, 1997.

(22) Leung, W.-H.; Zheng, H. G.; Chim, J. L. C.; Chan, J.; Wong, W.-T.; Williams, I. D. *J. Chem. Soc., Dalton Trans.* **2000**, 423.

Table 1. Crystallographic Data and Experimental Details for Ru(tpip)₂(PPh₃)₂Cl(4-*t*-BuC₆H₄CN) (2), Ru(tpip)₂(PPh₃)₂Cl(SO₂) (3), *fac*-[Ru(NH₃)₃(PPh₃)₂Cl][tpip] (4), K₂Ru₂(tpip)₄(CO)₄Cl₂ (5), *cis*-Ru(tpip)₂(MeCN)Cl·CH₂Cl₂ (6·CH₂Cl₂), *cis*-Ru(tpip)₂(H₂O)Cl (7), and *cis*-Ru(tpip)₂(CHPh)PCy₃·1/2Et₂O (9·1/2Et₂O)

	2	3	4	5	6·CH ₂ Cl ₂	7	9·1/2Et ₂ O
formula	C ₇₁ H ₆₅ ClN ₂ O ₂ P ₄ Ru	C ₆₀ H ₅₀ ClN ₄ O ₄ P ₄ RuS	C ₆₀ H ₅₀ ClN ₄ O ₂ P ₄ Ru	C ₁₀₀ H ₈₀ Cl ₂ K ₂ N ₄ O ₁₂ P ₈ Ru ₂	C ₅₁ H ₄₅ Cl ₃ N ₃ O ₄ P ₄ Ru	C ₄₈ H ₄₂ ClN ₂ O ₃ P ₄ Ru	C ₇₅ H ₈₄ N ₂ O _{4.50} P ₅ Ru
fw	1236.63	1141.47	1128.51	2128.86	1095.20	987.24	1341.36
crystal system	monoclinic	triclinic	monoclinic	triclinic	monoclinic	monoclinic	monoclinic
space group	<i>P</i> ₂ / <i>1</i> / <i>n</i>	<i>P</i> ₁	<i>P</i> ₂ / <i>1</i> / <i>c</i>	<i>P</i> ₁	<i>P</i> ₂ / <i>1</i> / <i>n</i>	<i>P</i> ₂ / <i>1</i> / <i>n</i>	<i>P</i> ₂ / <i>1</i> / <i>n</i>
<i>a</i> (Å)	13.4407(7)	12.0580(11)	10.7566(8)	11.6657(6)	11.2502(2)	11.3808(15)	13.9898(9)
<i>b</i> (Å)	19.6714(11)	12.8985(12)	19.3921(14)	14.1758(7)	25.2344(4)	32.987(4)	22.1110(15)
<i>c</i> (Å)	22.9195(13)	19.6961(19)	25.8888(19)	16.6971(8)	17.5564(3)	12.6875(16)	21.8982(18)
α (deg)		78.641(2)		100.351(1)			
β (deg)	91.753(1)	72.408(2)	99.3200(10)	104.048(1)	97.050(1)	112.504(2)	92.172(3)
γ (deg)	63.987(2)	63.987(2)	5328.9(7)	110.551(1)	4946.44(14)	4400.4(10)	6768.9(8)
<i>V</i> (Å ³)	6057.0(6)	2616.8(4)	4	2399.1(2)	4	4	4
ρ_{calc} (g cm ⁻³)	1.356	1.449	1.407	1.473	1.471	1.490	1.316
<i>T</i> (K)	100(2)	100(2)	100(2)	100(2)	100(2)	100(2)	100(2)
<i>F</i> (000)	2560	1172	2336	1084	2236	2020	2812
μ (mm ⁻¹)	0.457	0.563	0.513	0.654	0.656	0.612	0.401
total refin	32199	13717	25912	21811	27262	21190	28421
indep. refin	10564	8880	9115	10579	8642	7613	11393
<i>R</i> _{int}	0.0310	0.0262	0.0329	0.0321	0.0434	0.0520	0.1051
GoF ^a	1.024	1.020	0.962	1.014	0.996	0.972	0.975
<i>R</i> ₁ , <i>wR</i> ₂ ^c [<i>I</i> > 2 σ (<i>I</i>)]	0.0310, 0.0733	0.0366, 0.0889	0.0337, 0.0647	0.0419, 0.0812	0.0365, 0.0814	0.0508, 0.1068	0.0665, 0.0922
<i>R</i> ₁ , <i>wR</i> ₂ ^c (all data)	0.0442, 0.0775	0.0417, 0.0914	0.0459, 0.0674	0.0538, 0.0856	0.0551, 0.0861	0.0740, 0.1134	0.1162, 0.1020

$$^a \text{GoF} = [\sum w(F_o - F_c)^2 / (N_{\text{obs}} - N_{\text{param}})]^{1/2}, \quad ^b R_1 = \sum |F_o| - |F_c| / \sum |F_o|, \quad ^c wR_2 = [\sum w(F_o - F_c)^2 / \sum w(F_o)^2]^{1/2}.$$

Table 2. Selected Bond Lengths (Å) and Angles (deg) for Ru(tpip)(PPh₃)₂Cl(X)

	X	
	4- <i>t</i> -Bu-C ₆ H ₄ CN (2)	SO ₂ (3)
Bond Lengths		
Ru(1)–O(1)	2.1611(15)	2.1613(16)
Ru(1)–O(2)	2.1557(14)	2.1185(17)
Ru(1)–P(3)	2.2895(6)	2.3314(7)
Ru(1)–P(4)	2.2866(6)	2.3473(7)
Ru(1)–Cl	2.3885(5)	2.3568(6)
Ru(1)–X	1.9792(17)	2.1326(6)
P(1)–O(1)	1.5046(15)	1.5135(18)
P(2)–O(2)	1.5110(15)	1.5209(18)
P(1)–N(2)/(1)	1.5963(19)	1.586(2)
P(2)–N(2)/(1)	1.593(2)	1.590(2)
Bond Angles		
O(1)–Ru(1)–O(2)	87.89(6)	91.35(6)
P(3)–Ru(1)–P(4)	101.24(2)	104.61(2)
O(1)–Ru(1)–P(3)	86.45(4)	172.15(5)
O(2)–Ru(1)–P(4)	84.41(4)	169.76(5)
O(1)–Ru(1)–P(4)	172.25(4)	83.17(5)
O(2)–Ru(1)–P(3)	174.29(4)	80.80(5)
Cl(1)–Ru(1)–X	167.98(5)	175.94(2)
Cl(1)–Ru(1)–O(1)	86.07(4)	86.27(5)
Cl(1)–Ru(1)–O(2)	87.48(4)	85.75(5)
Cl(1)–Ru(1)–P(3)	92.863(19)	93.23(2)
Cl(1)–Ru(1)–P(4)	94.50(2)	85.27(2)
X–Ru(1)–O(1)	82.80(6)	89.72(5)
X–Ru(1)–O(2)	87.60(6)	94.94(5)
X–Ru(1)–P(3)	90.96(5)	90.83(2)
X–Ru(1)–P(4)	95.93(5)	93.69(2)
P(1)–N(2)/(1)–P(2)	122.69(11)	123.47(14)

Table 3. Selected Bond Lengths (Å) and Angles (deg) for *fac*-[Ru(NH₃)₃(PPh₃)₂Cl][tpip] (4)

Bond Lengths			
Ru(1)–N(1)	2.190(2)	Ru(1)–N(2)	2.1659(18)
Ru(1)–N(3)	2.1132(18)	Ru(1)–Cl(4)	2.4572(6)
Ru(1)–P(1)	2.3204(6)	Ru(1)–P(2)	2.2844(7)
P(3)–N(10)	1.576(2)	P(4)–N(10)	1.584(2)
P(3)–O(2)	1.5012(17)	P(4)–O(1)	1.5005(17)
Bond Angles			
Cl(1)–Ru(1)–N(1)	90.67(5)	Cl(1)–Ru(1)–N(2)	82.31(5)
Cl(1)–Ru(1)–N(3)	167.38(5)	Cl(1)–Ru(1)–P(1)	98.48(2)
Cl(1)–Ru(1)–P(2)	89.57(2)	P(1)–Ru(1)–N(1)	87.58(5)
P(1)–Ru(1)–N(2)	167.41(6)	P(1)–Ru(1)–N(3)	93.82(5)
P(1)–Ru(1)–P(2)	101.68(2)	P(2)–Ru(1)–N(1)	170.60(5)
P(2)–Ru(1)–N(2)	90.88(6)	P(2)–Ru(1)–N(3)	90.73(6)
N(1)–Ru(1)–N(2)	79.84(7)	N(1)–Ru(1)–N(3)	87.00(7)
N(2)–Ru(1)–N(3)	85.07(7)	P(3)–N(10)–P(4)	141.86(14)

formation of the triammine complex *fac*-[Ru(NH₃)₃(PPh₃)₂Cl]-[tpip] (4), which contains a tpip[−] counteranion. The ease of displacement of the tpip[−] ligand in **1** by NH₃ indicates that the interaction between Ru(II) and the hard tpip[−] ligand is not strong. The ³¹P{¹H} NMR spectrum of **2** showed two doublets at δ 23.97 and 51.18 (³*J*_{PP} = 3.3 Hz) that were assigned to the tpip[−] and PPh₃ ligands, respectively. The corresponding signals for **3** appeared as two singlets at δ 27.34 and 32.36. The NMR data for **2** and **3** are consistent with their solid-state structures (see below), in which the two PPh₃ are *cis* to each other and *trans* to the tpip[−] ligand. The ³¹P{¹H} NMR spectrum of **4** showed two singlets at δ 11.0 and 50.69 that were assigned to the tpip[−] anion and the PPh₃ ligands, respectively, consistent with the solid-state structure.

Reaction of [Ru(CO)₂Cl₂]_x with 2 equiv of K(tpip) in refluxing THF afforded the K/Ru bimetallic compound

Table 4. Selected Bond Lengths (Å) and Angles (deg) for $K_2Ru_2(tpip)_4(CO)_4Cl_2$ (**5**)

Bond Lengths			
Ru(1)–C(1)	1.858(3)	Ru(1)–C(2)	1.849(3)
Ru(1)–O(1)	2.1341(16)	Ru(1)–O(2)	2.0949(16)
Ru(1)–O(3)	2.1277(17)	Ru(1)–Cl(1)	2.3820(6)
K(1A)–O(1)	2.6988(17)	K(1A)–O(3)	2.8039(17)
K(1A)–O(4)	2.7051(19)	K(1)–O(4)	2.6288(17)
K(1A)–Cl(1)	3.1915(8)	N(1)–P(1)	1.585(2)
N(1)–P(2)	1.595(2)	N(2)–P(3)	1.583(2)
N(2)–P(4)	1.602(2)	P(1)–O(1)	1.5275(17)
P(2)–O(2)	1.5359(17)	P(3)–O(3)	1.5247(18)
P(4)–O(4)	1.5050(18)		
Bond Angles			
C(1)–Ru(1)–C(2)	85.65(11)	C(1)–Ru(1)–O(1)	96.72(9)
C(1)–Ru(1)–O(2)	96.81(9)	C(1)–Ru(1)–O(3)	177.84(9)
C(1)–Ru(1)–Cl(1)	89.01(8)	C(2)–Ru(1)–O(1)	177.62(9)
C(2)–Ru(1)–O(2)	90.20(8)	C(2)–Ru(1)–O(3)	94.98(9)
C(2)–Ru(1)–Cl(1)	96.22(7)	O(1)–Ru(1)–O(2)	89.43(6)
O(1)–Ru(1)–O(3)	82.65(6)	O(1)–Ru(1)–Cl(1)	83.93(5)
O(2)–Ru(1)–O(3)	85.25(6)	O(2)–Ru(1)–Cl(1)	171.65(5)
O(3)–Ru(1)–Cl(1)	88.87(5)	Cl(1)–K(1A)–O(1)	61.14(4)
Cl(1)–K(1A)–O(3)	63.28(4)	Cl(1)–K(1A)–O(4)	142.75(4)
Cl(1)–K(1A)–O(4A)	114.86(4)	O(1)–K(1A)–O(3)	61.48(5)
O(1)–K(1A)–O(4)	126.95(6)	O(1)–K(1A)–O(4A)	133.44(6)
O(3)–K(1A)–O(4)	88.07(5)	O(3)–K(1A)–O(4A)	163.58(6)
O(4)–K(1A)–O(4A)	85.73(6)	Ru(1)–C(1)–O(10)	174.6(2)
Ru(1)–C(2)–O(20)	177.1(2)	P(1)–N(1)–P(2)	126.13(13)
P(3)–N(2)–P(4)	132.71(14)		

Table 5. Selected Bond Lengths (Å) and Angles (deg) for $cis-Ru(tpip)_2(X)Cl$

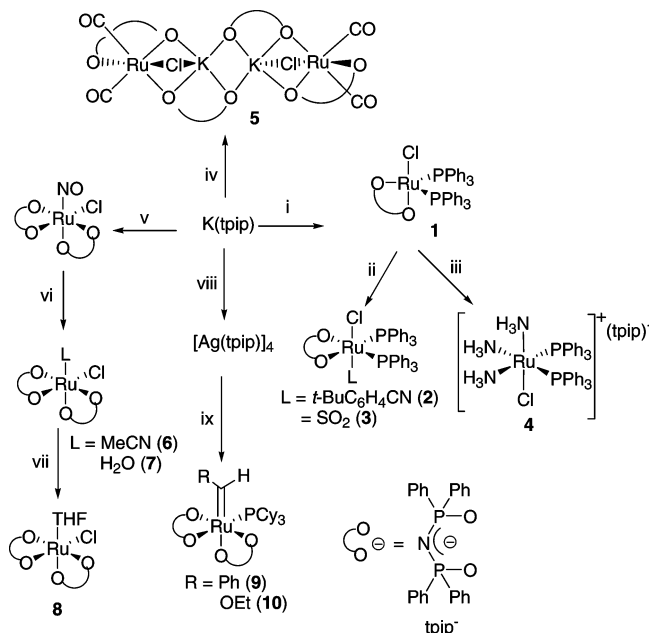
	X	
	MeCN (6)	H ₂ O (7)
Bond Lengths		
Ru(1)–O(1)	2.0523(19)	2.048(3)
Ru(1)–O(2)	2.0262(19)	2.033(3)
Ru(1)–O(3)	2.0265(19)	2.018(3)
Ru(1)–O(4)	2.0272(19)	2.046(3)
Ru–Cl	2.3034(7)	2.3294(11)
Ru–X	2.002(3)	2.060(3)
P(1)–O(1)	1.522(2)	1.513(3)
P(2)–O(2)	1.526(2)	1.520(3)
P(1)–N(1)	1.583(3)	1.590(4)
P(2)–N(1)	1.583(3)	1.583(4)
P(3)–O(3)	1.521(2)	1.527(3)
P(4)–O(4)	1.528(2)	1.535(3)
P(3)–N(2)	1.590(2)	1.581(4)
P(4)–N(2)	1.579(2)	1.574(4)

Bond Angles		
O(1)–Ru(1)–O(2)	90.31(8)	92.27(11)
O(1)–Ru(1)–O(3)	84.40(8)	90.19(12)
O(1)–Ru(1)–O(4)	87.24(8)	88.38(11)
O(1)–Ru(1)–X	95.14(9)	88.38(12)
O(1)–Ru(1)–Cl(1)	175.30(6)	177.83(9)
O(2)–Ru(1)–O(3)	85.74(8)	88.87(11)
O(2)–Ru(1)–O(4)	177.47(8)	174.63(11)
O(2)–Ru(1)–X	89.47(9)	88.78(11)
O(2)–Ru(1)–Cl(1)	91.52(6)	89.45(8)
O(3)–Ru(1)–O(4)	94.60(8)	96.46(11)
O(3)–Ru(1)–X	175.19(9)	177.19(11)
O(3)–Ru(1)–Cl(1)	91.42(6)	91.17(9)
O(4)–Ru(1)–X	90.16(9)	85.91(11)
O(4)–Ru(1)–Cl(1)	90.97(6)	89.78(8)
X–Ru–Cl(1)	89.20(7)	90.33(9)
P(1)–N(1)–P(2)	127.44(16)	126.1(2)
P(3)–N(2)–P(4)	129.43(16)	130.1(2)

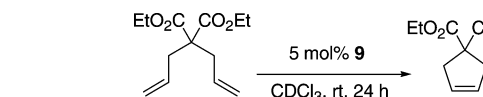
$K_2Ru_2(tpip)_4(CO)_4Cl_2$ (**5**), which was isolated as pale-yellow crystals. **5** is air-sensitive in solutions and readily turns gray upon exposure to air. The IR spectrum of **5** showed two ν_{CO} bands at 1974 and 2051 cm^{-1} , which are comparable to those

Table 6. Selected Bond Lengths (Å) and Angles (deg) for $cis-Ru(tpip)_2(ChPh)(PCy_3)$ (**9**)

Bond Lengths			
Ru(1)–C(1)	1.864(5)	Ru(1)–O(1)	2.103(3)
Ru(1)–O(2)	2.173(3)	Ru(1)–O(3)	2.110(3)
Ru(1)–O(4)	2.242(3)	Ru(1)–P(5)	2.3397(13)
P(1)–O(1)	1.522(3)	P(2)–O(2)	1.516(3)
P(3)–O(3)	1.533(3)	P(4)–O(4)	1.516(3)
N(1)–P(1)	1.590(4)	N(1)–P(2)	1.601(4)
N(2)–P(3)	1.591(4)	N(2)–P(4)	1.584(4)
Bond Angles			
O(1)–Ru(1)–O(2)	89.73(11)	O(3)–Ru(1)–O(4)	90.44(11)
O(1)–Ru(1)–O(3)	170.67(11)	O(1)–Ru(1)–O(4)	81.36(11)
O(2)–Ru(1)–O(3)	85.24(12)	O(2)–Ru(1)–O(4)	86.09(11)
C(1)–Ru(1)–O(1)	89.41(17)	C(1)–Ru(1)–O(2)	91.22(16)
C(1)–Ru(1)–O(3)	98.54(17)	C(1)–Ru(1)–O(4)	170.39(16)
C(1)–Ru(1)–P(5)	88.54(14)	P(5)–Ru(1)–O(1)	93.21(9)
P(5)–Ru(1)–O(2)	177.05(9)	P(5)–Ru(1)–O(3)	91.89(9)
P(5)–Ru(1)–O(4)	94.62(9)	P(1)–N(1)–P(2)	122.2(3)
P(3)–N(2)–P(4)	127.9(2)		

Scheme 1. Syntheses of Ru(tpip) Complexes^a


^a (i) $Ru(PPh_3)_3Cl_2$, THF, reflux; (ii) L, CH_2Cl_2 , RT; (iii) $NH_3(g)$, CH_2Cl_2 , RT; (iv) $[Ru(CO)_2Cl_2]_x$, THF, reflux; (v) $Ru(NO)Cl_3 \cdot xH_2O$, acetone, reflux (ref 16); (vi) $h\nu$, L/CH_2Cl_2 ; (vii) THF, reflux; (viii) $AgNO_3$, MeOH, RT (ref 9a); (ix) $Ru(=CHR)(PCy_3)_2Cl_2$.

Scheme 2. Ru-Catalyzed RCM of Diethyl Diallylmalonate


of $cis-Ru(acac)_2(CO)_2$ (1988 and 2057 cm^{-1})²³ and $Ru(L_{OEt})(CO)_2Cl$ ($L_{OEt} = [(\eta^5-C_5H_5)Co\{P(O)(OEt)_2\}_3]^-$) (1964 and 2044 cm^{-1}).²⁴ The $^{31}P\{^1H\}$ NMR spectrum displayed two doublets at δ 30.52 and 33.58 ($J = 3.6$ Hz), which were tentatively assigned to the κ_2 -tpip[−] ligands, and two broad singlets at δ 13.95 and 22.03, which were attributed to the κ_1 -tpip[−] ligands (refer to the solid-state structure of **5** described below).

B. Ru(III) Complexes. Previously, we reported the synthesis of photoactive $Ru\{N(Ph_2PQ)\}_2(NO)Cl$ from $Ru(NO)-$

(23) Calderazzo, F.; Floriani, C.; Henzi, R.; L'Eplattenier, F. *J. Chem. Soc. A* **1969**, 1378.

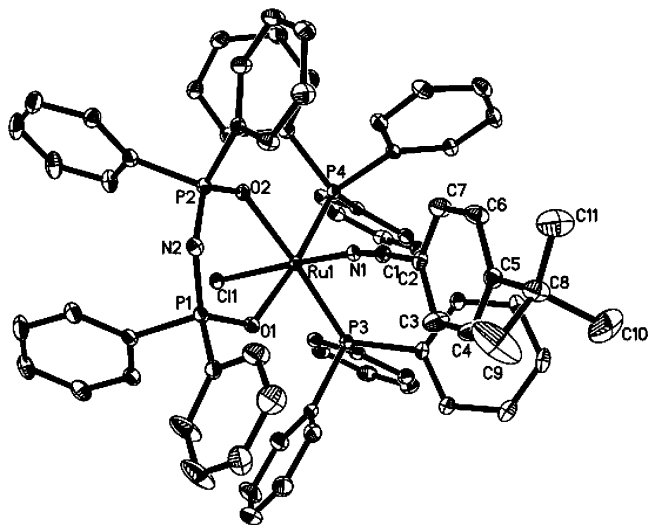


Figure 1. Molecular structure of $\text{Ru}(\text{tpip})_2(\text{PPh}_3)_2\text{Cl}(4\text{-}t\text{-Bu-C}_6\text{H}_4\text{CN})$ (**2**). The ellipsoids are drawn at the 30% probability level.

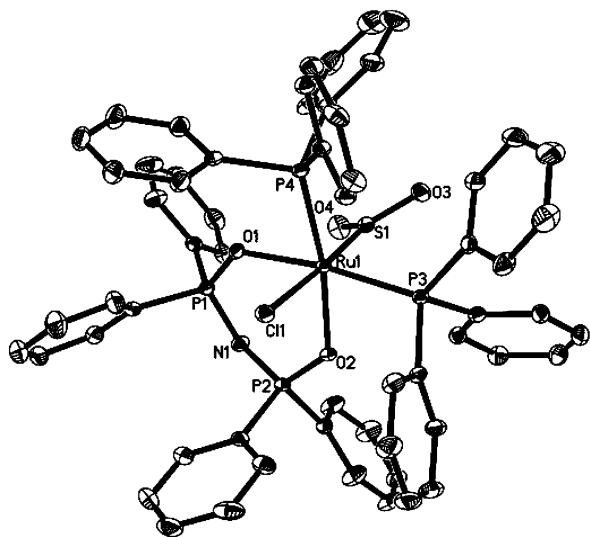


Figure 2. Molecular structure of $\text{Ru}(\text{tpip})_2(\text{PPh}_3)_2\text{Cl}(\text{SO}_2)$ (**3**). The ellipsoids are drawn at the 30% probability level.

Cl_3L_2 ($\text{L} = \text{PPh}_3$ or H_2O) and $\text{K}[\text{N}(\text{Ph}_2\text{PQ})_2]$ ($\text{Q} = \text{O}, \text{S}, \text{Se}$).¹⁶ Irradiation of CH_2Cl_2 solutions of $\text{Ru}\{\text{N}(\text{Ph}_2\text{PQ})\}_2(\text{NO})\text{Cl}$ ($\text{Q} = \text{S}, \text{Se}$) using UV light led to release of NO. Unfortunately, we were not able to crystallize the Ru(III) photoproducts for structural characterization. In this work, we found that photolysis of *cis*- $\text{Ru}(\text{tpip})_2(\text{NO})\text{Cl}$ in $\text{CH}_2\text{Cl}_2/\text{MeCN}$ gave *cis*- $\text{Ru}(\text{tpip})_2(\text{MeCN})\text{Cl}$ (**6**), which could be isolated as air-stable crystals. Similarly, the aqua compound *cis*- $\text{Ru}(\text{tpip})_2\text{Cl}(\text{H}_2\text{O})$ (**7**) was prepared by photolysis of *cis*- $\text{Ru}(\text{tpip})_2(\text{NO})\text{Cl}$ in wet CH_2Cl_2 . Compound **6** is paramagnetic, with a measured magnetic moment of $1.7\mu_{\text{B}}$ that is consistent with an $S = 1/2$ spin state. No reaction was found when **6** was refluxed with excess pyridine (10-fold) in CH_2Cl_2 for 2 h. Refluxing **6** in neat THF overnight led to isolation of an orange solid characterized as $\text{Ru}(\text{tpip})_2(\text{THF})\text{Cl}$ (**8**). Attempts to prepare $\text{Ru}(\text{tpip})_3$ by reaction of **6** or **8** with 1 equiv of $\text{K}(\text{tpip})$ in CH_2Cl_2 failed.

C. Ru(IV) Complexes. No reaction was found between $\text{Ru}(\text{CHPh})\text{Cl}_2(\text{PCy}_3)_2$ and $\text{K}(\text{tpip})$. The carbene complex *cis*- $\text{Ru}(\text{tpip})_2(\text{CHPh})(\text{PCy}_3)$ (**9**) could be isolated as air-stable

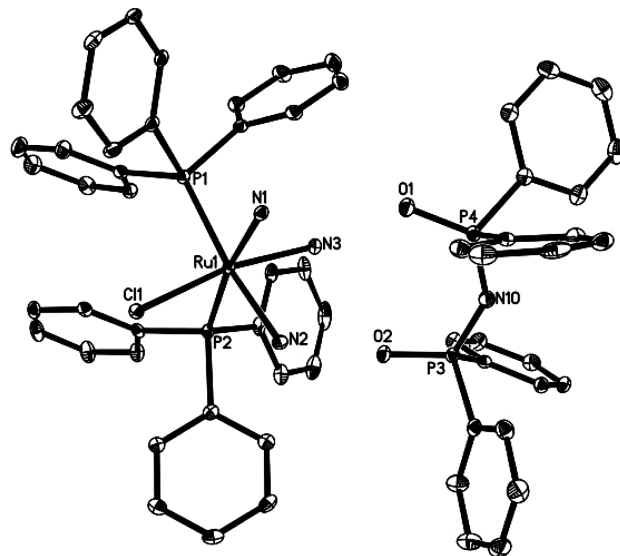


Figure 3. Molecular structure of *fac*- $[\text{Ru}(\text{NH}_3)_3(\text{PPh}_3)_2\text{Cl}][\text{tpip}]$ (**4**). The ellipsoids are drawn at the 30% probability level.

green crystals by reaction of $\text{Ru}(\text{CHPh})\text{Cl}_2(\text{PCy}_3)_2$ with $[\text{Ag}(\text{tpip})]_4$. An analogous Fischer carbene complex, *cis*- $\text{Ru}(\text{tpip})_2(\text{CHOEt})(\text{PCy}_3)$ (**10**), was prepared similarly from $\text{Ru}(\text{CHOEt})\text{Cl}_2(\text{PCy}_3)_2$ and $[\text{Ag}(\text{tpip})]_4$. It should be noted that reaction of $\text{Ru}(\text{CHPh})\text{Cl}_2(\text{PCy}_3)_2$ with $\text{K}[\text{N}(\text{Ph}_2\text{PS})_2]$ afforded five-coordinate $\text{Ru}[\text{N}(\text{Ph}_2\text{PS})_2]_2(\text{CHPh})$, whereas reaction with $\text{K}[\text{N}(\text{Ph}_2\text{PSe})_2]$ led to formation of a mixture of $\text{Ru}[\text{N}(\text{Ph}_2\text{PSe})_2]_2(\text{CHPh})$ and $\text{Ru}[\text{N}(\text{Ph}_2\text{PSe})_2][\text{PhP}(\text{Se})\text{NPPH}_2](\text{CHPh})$, the latter of which contains a monoselenide ligand.²⁵ In contrast, compound **9** is six-coordinate and contains a PCy_3 ligand. The $^3\text{P}\{^1\text{H}\}$ NMR spectrum of **9** showed four multiplets at δ 21.84, 26.75, 27.17, and 34.85 due to the two mutually *cis* tpip^- ligands as well as a singlet at δ 28.06 attributable to PCy_3 . The signal from the carbene proton ($\text{Ru}=\text{CHPh}$) appeared as a doublet at δ 22.46 ($^3J_{\text{PH}} = 7.5$ Hz) located further downfield than that of $\text{Ru}[\text{N}(\text{Ph}_2\text{PS})_2]_2(\text{CHPh})$ (δ 18.16).²⁵ The corresponding resonance for **10** was found further upfield (δ 16.62). The ^{13}C chemical shifts for the carbene carbons in **9** and **10** (δ 295.07 and 290.60, respectively) are typical of Ru(IV) carbene complexes.

Complex **9** is capable of catalyzing ring-closing metathesis (RCM) of dienes, although its catalytic activity is considerably less than that of Grubbs' catalyst, presumably because it is coordinately saturated. For example, RCM of diethyl diallylmalonate in the presence 5 mol % of **9** was complete in 24 h (Scheme 2).

Crystal Structures. The molecular structures of **2** and **3** are shown in Figures 1 and 2, respectively. Selected bond lengths and angles are compiled in Table 2. In each complex, the geometry around Ru is pseudo-octahedral, with the two PPh_3 ligands trans to tpip^- . The average Ru–O and Ru–P distances in **2** (2.158 and 2.288 Å, respectively) and **3** (2.1399 and 2.3394 Å, respectively) are comparable to those

(24) Leung, W.-H.; Chan, E. Y. Y.; Wong, W.-T. *Inorg. Chem.* **1999**, *38*, 136.

(25) Leung, W.-H.; Lau, K.-K.; Zhang, Q.-F.; Wong, W.-T.; Tang, B. *Organometallics* **2000**, *19*, 2084.

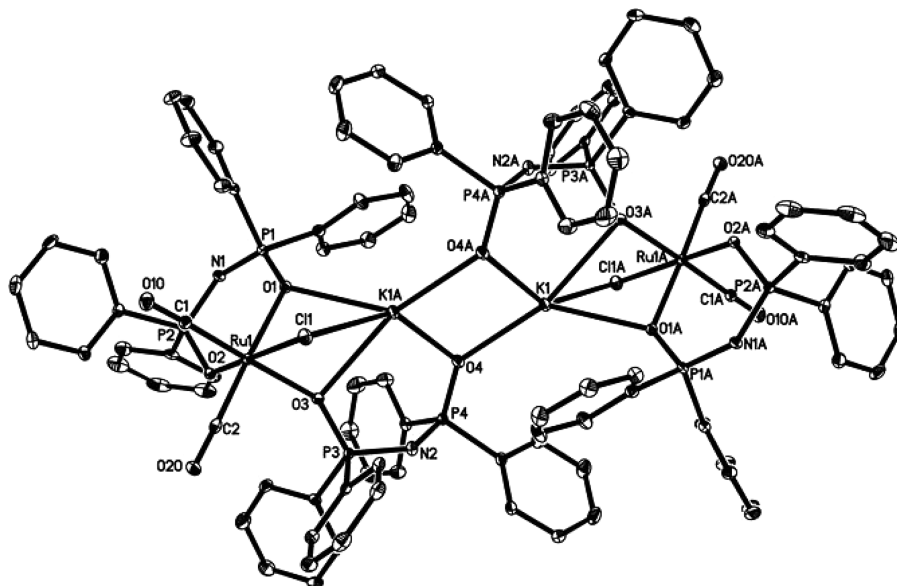


Figure 4. Molecular structure of $\text{K}_2\text{Ru}_2(\text{tpip})_4(\text{CO})_4\text{Cl}_2$ (**5**). The ellipsoids are drawn at the 30% probability level.

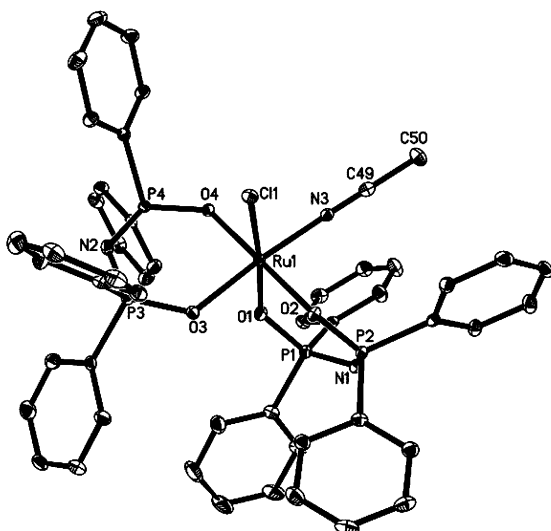


Figure 5. Molecular structure of *cis*- $\text{Ru}(\text{tpip})_2(\text{MeCN})\text{Cl}$ (**6**). The ellipsoids are drawn at the 30% probability level.

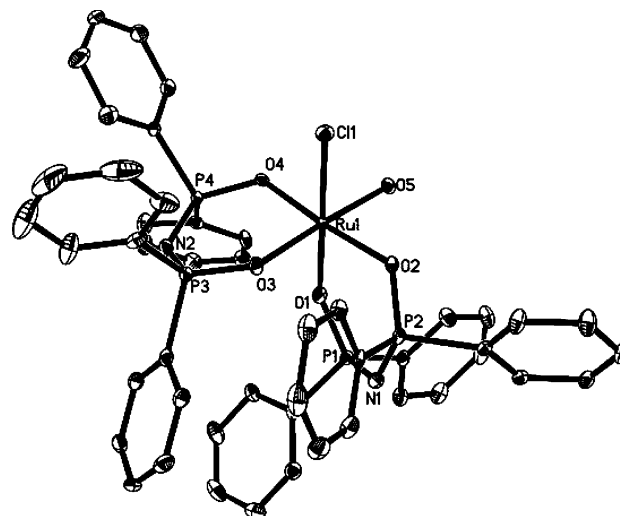


Figure 6. Molecular structure of *cis*- $\text{Ru}(\text{tpip})_2(\text{H}_2\text{O})\text{Cl}$ (**7**). The ellipsoids are drawn at the 30% probability level.

of $\text{Ru}(\text{LOEt})(\text{PPh}_3)_2\text{Cl}$ (2.183 and 2.267 Å, respectively).^{3a} The Ru–Cl distance in **3** [2.3568(6) Å] is slightly shorter than that in **2** [2.3885(5) Å]. The SO_2 ligand in **3** binds to Ru in a planar fashion (sum of bond angles of S = 360°). The Ru–S distance of 2.1326(6) Å in **3** is similar to that in *cis*- $\text{Ru}[\text{N}(\text{Ph}_2\text{PS})_2]_2(\text{PPh}_3)(\text{SO}_2)$ [2.140(4) Å].²²

The molecular structure of **4** is shown in Figure 3; selected bond lengths and angles are listed in Table 3. The geometry around Ru is pseudo-octahedral with three facially coordinated NH_3 ligands. The average Ru–N distance of 2.156 Å is slightly shorter than that in $[\text{Ru}(\text{NH}_3)_5(\text{Me}_2\text{SO})][\text{PF}_6]_2$ (2.217 Å).²⁶ The Ru–N bonds trans to PPh_3 [2.190(2) and 2.1659(18) Å] are longer than that trans to Cl [2.1132(18) Å] as a result of the trans influence of PPh_3 .

Figure 4 shows the molecular structure of **5**; selected bond lengths and angles are listed in Table 4. Compound **5** can be viewed as consisting of two symmetry-related $\{\text{KRu}(\kappa_2$ -

$\text{tpip})(\kappa_1\text{-tpip})(\text{CO})_2\text{Cl}\}$ fragments linked together via two K–O bridges. In each fragment, the Ru has pseudo-octahedral geometry with two mutually cis carbonyls. The Ru–O bonds trans to the CO ligands [2.1341(16) and 2.1277(17) Å] are longer than that trans to Cl [2.0949(16) Å] because of the trans influence of the carbonyl group. The K atom is five-coordinate, binding to the chloride, one oxygen atom of the κ_2 -tpip[−] ligand, both oxygen atoms of the κ_1 -tpip[−] ligand, and one oxygen atom of the κ_2 -tpip[−] ligand in the adjacent fragment. The K–O distances are in the range 2.6988(17)–2.8039(17) Å. The K–Cl distance is rather long [3.1915(8) Å], indicating that the K–Cl interaction is weak.

The structures of **6** and **7** are shown in Figures 5 and 6, respectively. Selected bond lengths and angles are compiled in Table 5. The geometry around Ru in each complex is pseudo-octahedral, with the acetonitrile/aqua ligand cis to the chloride. The average Ru–O distance and the Ru–Cl distance in **6** [2.033 and 2.3034(7) Å, respectively] and **7**

(26) March, F. C.; Ferguson, G. *Can. J. Chem.* **1971**, *49*, 3590.

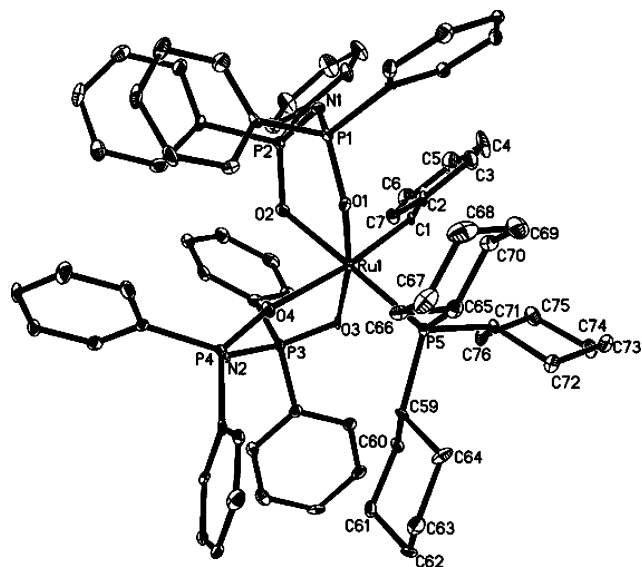


Figure 7. Molecular structure of *cis*-Ru(tpip)₂(CHPh)(PCy₃) (**9**). The ellipsoids are drawn at the 30% probability level.

Table 7. Formal Potentials ($E_{1/2}$) for Ru(tpip) Complexes^a

complex	$E_{1/2}$ (V vs Cp ₂ Fe ⁺⁰)	
	reduction	oxidation
Ru(tpip)(PPh ₃) ₂ Cl(4- <i>t</i> -Bu-C ₆ H ₄ CN) (2)		0.16
Ru(tpip)(PPh ₃) ₂ Cl(SO ₂) (3)		0.63 ^c
<i>cis</i> -Ru(tpip) ₂ (NO)Cl	−1.54 ^b	
<i>trans</i> -Ru[N(Ph ₂ PS) ₂] ₂ (NO)Cl	−1.15 ^b	
<i>cis</i> -Ru(tpip) ₂ (MeCN)Cl (6)	−1.07	0.84
<i>cis</i> -Ru(tpip) ₂ (H ₂ O)Cl (7)	−1.20	0.66
<i>cis</i> -Ru(tpip) ₂ (THF)Cl (8)	−1.47 ^b	0.56
<i>cis</i> -Ru(tpip) ₂ (CHPh)PCy ₃ (9)		−0.05
<i>cis</i> -Ru(tpip) ₂ (CHOEt)PCy ₃ (10)		−0.24
Ru[N(Ph ₂ PS) ₂] ₂ (CHPh)		0.05

^a Potentials were measured at a glassy carbon electrode in CH₂Cl₂ solutions containing 0.1 M [*n*-Bu₄N][PF₆] as the supporting electrolyte using a scan rate of 100 mV s^{−1}. ^b Irreversible, E_{pc} value. ^c Irreversible, E_{pa} value.

[2.036 and 2.3294(11) Å, respectively] are shorter than those in the Ru(II) compounds **2** and **3**, as a result of the smaller ionic radius of Ru³⁺ as opposed to Ru²⁺. The Ru–O(aquo) distance of 2.060(3) Å in **7** is similar to the average [2.029(7) Å] of those in [Ru(H₂O)₆](OTs)₃ (TsO[−] = *p*-toluenesulfonate).²⁷ The Ru–O(tpip) distances in the Ru(III) complexes were found to increase in the order Ru–O(trans to H₂O) [2.018(3) Å] < Ru–O(trans to P=O) [2.0262(19)–2.046(3) Å] < Ru–O(trans to Cl) [2.048(3) Å] < Ru–O(trans to MeCN) [2.0625(19) Å], which is suggestive of the order of the trans influences, H₂O < tpip[−] < Cl[−] < MeCN.

Figure 7 shows the molecular structure of **9**; selected bond lengths and angles are listed in Table 6. The geometry around Ru is pseudo-octahedral, with the benzylidene and PCy₃ ligands adjacent to each other. The Ru–C [1.864(5) Å] and Ru–P [2.3397(13) Å] distances are comparable to those in [Ru(=CHPh)(Tp)(PCy₃)(H₂O)][PF₆] [Tp[−] = hydridotris(pyrazolyl)borate] [1.878(4) and 2.3822(13) Å, respectively].¹⁹ The Ru–O distances were found to increase in the order Ru–O(trans to P=O) (average of 2.107 Å) < Ru–O(trans to P) [2.173(3) Å] < Ru–O(trans to carbene) [2.242(3) Å],

Table 8. Ru-Catalyzed Oxidation of Alcohols^a

entry	catalyst	alcohol	oxidant	time (h)	product (% yield ^b)
1	1	PhCH ₂ OH	TBHP	2	PhCHO (67)
2	1	PhCH ₂ OH	NMO	1.5	PhCHO (98)
3	5	PhCH ₂ OH	TBHP	2	PhCHO (49)
4	5	PhCH ₂ OH	NMO	2	PhCHO (67)
5	6	PhCH ₂ OH	NMO	1	PhCHO (9)
6	7	PhCH ₂ OH	NMO	2	PhCHO (66)
7	9	PhCH ₂ OH	TBHP	3	PhCHO (93)
8	9	PhCH ₂ OH	NMO	1	PhCHO (100)
9	1	PhCH(OH)Me	NMO	2	PhC(O)Me (82)
10	5	PhCH(OH)Me	NMO	2	PhC(O)Me (54)
11	7	PhCH(OH)Me	NMO	1.5	PhC(O)Me (64)
12	9	PhCH(OH)Me	NMO	2	PhC(O)Me (83)
13	9	cyclohexanol	NMO	2	cyclohexanone (80)

^a Experimental conditions: a mixture of alcohol (0.2 mmol), oxidant (0.2 mmol), and catalyst (0.002 mmol, 1 mol %) in CH₂Cl₂ (2 mL) was stirred at room temperature under nitrogen. ^b Yield based on the amount of oxidant used.

Table 9. Ru-Catalyzed Oxidation of Olefins^a

entry	catalyst	substrate	time (h)	products (% yield ^b)
1	1	styrene	3	styrene oxide (6), benzaldehyde (7)
2	7	styrene	3	benzaldehyde (3)
3	9	styrene	2	styrene oxide (35), benzaldehyde (15)
4	10	styrene	2	styrene oxide (31), benzaldehyde (12)
5	9	cyclohexene	2	cyclohexene oxide (45), cyclohexanone (trace)
6	9	cyclooctene	2	cyclooctene oxide (58)
7	9	<i>cis</i> -stilbene	2	<i>cis</i> -stilbene oxide (40)

^a Experimental conditions: a mixture of olefin (0.2 mmol), iodosylbenzene (0.20 mmol), and catalyst (0.002 mmol, 1 mol %) in CH₂Cl₂ (2 mL) was stirred at room temperature under nitrogen. ^b Yield based on the amount of PhI formed.

reflecting the trend of the trans influences, tpip[−] < PCy₃ < carbene.

Electrochemistry. Formal potentials of the Ru(tpip) complexes were determined using cyclic voltammetry (Table 7). The cyclic voltammogram (CV) of **2** in CH₂Cl₂ showed a reversible couple at 0.16 V versus Cp₂Fe⁺⁰, which was assigned to the metal-centered Ru(III/II) couple. Under the same conditions, the ligand K(tpip) was redox-inactive in the potential range −2.0 to 1.0 V. Compound **3** exhibited an irreversible oxidation wave at 0.63 V, indicating that the Ru(II) state is stabilized by the π -acidic SO₂ ligand. No couples were observed for the dicarbonyl complex **5**. The CV for *cis*-Ru(tpip)₂(NO)Cl displayed an irreversible wave at −1.54 V that was tentatively assigned to the Ru(II/I) reduction. The reduction for *trans*-Ru(NO){N(Ph₂PS)₂}₂Cl occurred at a less-negative potential (−1.15 V), suggesting that the thiophosphinate ligand is more capable of stabilizing the Ru(I) state than is the P=O analogue. **6** exhibited two reversible redox couples at −1.07 and 0.84 V that were assigned to the Ru(III/II) and Ru(IV/III) couples, respectively. Although the acac[−] analogue of **6** is unknown, the Ru(III/II) potential for *cis*-Ru(acac)₂(MeCN)Cl may be assumed to lie between those of *trans*-[Ru(acac)₂Cl₂][−] and *cis*-Ru(acac)₂(MeCN)₂, which were determined to be −0.45 and 0.26 V versus the normal hydrogen electrode, respectively^{12a} (approximately −1.12 and −0.41 V vs Cp₂Fe⁺⁰ in

(27) Bernhard, P.; Bürgi, H.-B.; Hauser, J.; Lehmann, H.; Ludi, A. *Inorg. Chem.* **1982**, *21*, 3936.

MeCN²⁸). Thus, the electrochemical data indicated that tpip^- is a stronger electron donor than acac^- . The Ru(IV/III) potentials for **7** and **8** were less anodic than that of **6**, suggesting that the O-donor ligands H_2O and THF are more capable of stabilizing the Ru(IV) state than is N-bound MeCN. Unlike that for **6** and **7**, the Ru(III/II) reduction for complex **8** at -1.47 V is irreversible. The CV of **9** displayed a reversible couple at -0.05 V, which was assigned as a metal-centered couple [formally, the Ru(V/IV) couple]. A more-negative potential was found for the Fischer carbene analogue **10** (-0.24 V). The Ru(V/IV) potential for $\text{Ru}[\text{N}(\text{Ph}_2\text{PS})_2]_2(\text{CHPh})$ (0.05 V) was similar to that for **9**, suggesting that for the Ru(IV) carbene system, the donor strength of tpip^- is comparable to that of the thiophosphinate analogue.

Ru-Catalyzed Oxidation. The catalytic activity of Ru(tpip) complexes in the oxidation of alcohols was studied, and the results are summarized in Table 8. Both mono- and bis(tpip) complexes of Ru can catalyze selective oxidation of benzyl alcohol and methylbenzyl alcohol to benzaldehyde and acetophenone, respectively, in moderate to good yield. *N*-Methylmorpholine *N*-oxide (NMO) appears to be a better terminal oxidant than *tert*-butylhydroperoxide (TBHP) for the catalytic alcohol oxidation. However, prolonged oxidation of benzyl alcohol using NMO led to formation of benzoic acid, whereas no overoxidation of benzyl alcohol was found using TBHP. The catalytic activity of the Ru(IV)–bis(tpip) complexes is comparable to that of the Ru(II) complex **1** but greater than that of the Ru(III) counterparts. Complex **6** is not an active oxidation catalyst, possibly because substitution at the low-spin d^5 Ru(III) center is slow. Ru(tpip) complexes can also catalyze oxidation of secondary aliphatic alcohols. For example, oxidation of cyclohexanol with NMO in the presence of 1 mol % of **9** afforded cyclohexanone in 80% yield.

The catalytic oxidation of olefins with iodosylbenzene and Ru(tpip) complexes was also studied (Table 9). For example, oxidation of styrene with 1 mol % of the Ru(IV) complex **9** afforded styrene oxide and benzaldehyde in 35 and 25% yield, respectively. A similar yield of styrene oxide was obtained using the Fischer carbene complex **10** as the catalyst. In contrast, the Ru(II) and Ru(III) complexes are less active in olefin epoxidation. The oxidation of cyclohexene, cyclooctene, and *cis*-stilbene with **9** afforded the corresponding epoxides as major products, indicating that the Ru(tpip) oxo-active species is a selective oxidant.

An attempt to isolate the active intermediate(s) for the Ru(tpip)-catalyzed oxidation was made. The reaction between **9** and iodosylbenzene was monitored by NMR spectroscopy. Treatment of **9** in CDCl_3 with 2 equiv of iodosylbenzene at

room temperature resulted in the formation of a brown species **11**, which could be isolated as an air-stable solid by addition of a large amount of hexane to the reaction mixture. The ^1H NMR spectrum of **11** showed the absence of the resonance at δ 22.46, indicating the loss of the carbene group. The $^{31}\text{P}\{^1\text{H}\}$ NMR spectrum of **11** displayed two singlets at δ 20.33 and 50.88. The resonance at δ 20.33, which is within the range found for diamagnetic Ru(tpip) complexes, was attributed to tpip^- ligand(s), whereas the one at δ 50.88 possibly was due to a coordinated PCy_3 (or OPCy_3) ligand (^{31}P resonances for uncomplexed PCy_3 and OPCy_3 were found at approximately δ 9.7 and 46.7, respectively). The ESI mass spectrum showed a molecular ion peak at m/z 933 corresponding to $[\text{Ru}(\text{tpip})_2]^+$. However, no signals due to Ru(tpip) species having a PCy_3 ligand were observed. Isolated **11** can oxidize benzyl alcohol and PPh_3 to give benzaldehyde and OPPh_3 in 35 and 41% yield, respectively, but no reaction was found between **11** and styrene, suggesting that a different Ru active species is responsible for the **9**-catalyzed epoxidation. On the basis of the above evidence, we believe that **11** is a high-valence Ru–bis(tpip) complex, possibly an oxo species containing a PCy_3 ligand. Unfortunately, despite many attempts, we were not able to obtain a crystalline sample of **11** for structure determination. Additional experimental work is required in order to identify the active species of the Ru-catalyzed oxidation.

Concluding Remarks. In summary, transmetalation of $\text{K}(\text{tpip})$ or $[\text{Ag}(\text{tpip})]_4$ with a variety of Ru chloride compounds has been studied. For the reactions of $\text{Ru}(\text{PPh}_3)_3\text{Cl}_2$ and $[\text{Ru}(\text{CO})_2\text{Cl}_2]_x$, only mono(κ_2 -tpip) complexes were isolated, indicating the reluctance of Ru(II) to bind four hard $\text{P}=\text{O}$ groups in the coordination sphere. Ru–bis(tpip) complexes could be synthesized using nitrosyl and carbene complexes of Ru as starting materials. Photolysis of *cis*- $\text{Ru}(\text{tpip})_2(\text{NO})\text{Cl}$ produced $\text{Ru}(\text{tpip})_2(\text{solv})\text{Cl}$ complexes that may serve as useful precursors to Ru(III)–bis(tpip) complexes. The cyclic voltammetry study showed that tpip^- is a stronger electron donor than acac^- . Thus, one may expect that higher-valence Ru(tpip) complexes should be easily accessible and may exhibit interesting chemistry. *cis*- $\text{Ru}(\text{tpip})_2(\text{CHPh})(\text{PCy}_3)$ can catalyze oxidation of alcohols and olefins with NMO and iodosylbenzene, respectively.

Acknowledgment. We thank Dr. Herman H. Y. Sung for solving the crystal structures. Financial support from the Hong Kong Research Grants Council (Project 602104) is gratefully acknowledged.

Supporting Information Available: Tables of crystal data, final atomic coordinates, anisotropic thermal parameters, and complete lists of bond lengths and angles for complexes **2–7** and **9** (in CIF format). This material is available free of charge via the Internet at <http://pubs.acs.org>.

IC800018D

(28) Assuming that the $\text{Cp}_2\text{Fe}^{+/0}$ couple in MeCN occurs at 0.665 V versus the normal hydrogen electrode (Gennett, T.; Milner, D. F.; Weaver, M. J. *J. Phys. Chem.* **1985**, *89*, 2789).